Vol. 18, No. 3 (2019) 1101-1118
Revista Mexicana de Ingeniería Química

NUMERICAL ANALYSIS OF CO_2 TRANSIENT BEHAVIOR IN THE GAS COOLER DURING VARIABLE START-UP CONDITIONS OF A TRANSCRITICAL REFRIGERATION SYSTEM

ANÁLISIS NUMÉRICO DEL COMPORTAMIENTO TRANSITORIO DEL CO_2 EN EL ENFRIADOR DE GAS DURANTE CONDICIONES VARIABLES DE ARRANQUE DE UN SISTEMA DE REFRIGERACIÓN TRANSCRÍTICO

J.F. Ituna-Yudonago[1], J.M. Belman-Flores[2*], F. Elizalde-Blancas[2], V. Pérez-García[2], O. García-Valladares[1], I. Carvajal-Mariscal[3]

[1]*Renewable Energies Institute of UNAM. Privada Xochicalco s/n, Temixco ZC. 62580, Morelos, Mexico*
[2]*Engineering Division, Campus Irapuato-Salamanca, University of Guanajuato. Salamanca-Valle de Santiago km 3.5+1.8, ZC. 36885, Mexico.*
[3]*Instituto Politécnico Nacional, ESIME, UPALM, Av. IPN s/n, CDMX 07738, Mexico.*

Received: September 7, 2018; Accepted:

Abstract

Transient behavior of CO_2 in the gas cooler during variable start-up conditions of a transcritical refrigeration system is numerically investigated. The analysis is based on three cases including cold and warm start-up with zero initial refrigerant mass flow rate, and warm start-up with nominal CO_2 mass flow rate. The numerical analysis is performed using a 3D model and simulations are carried out using CFD code FLUENT. Effects of the transient change in the gas cooler inlet boundary conditions on the CO_2 temperature, mass flow rate, thermophysical properties, heat transfer parameters and thermal effectiveness are analyzed. Results show that, when the refrigeration system starts at high temperature and nominal refrigerant mass flow rate, the maximum thermal effectiveness of the gas cooler is 85%. When it starts at high temperature, with zero initial mass flow rate, the thermal effectiveness decreases up to 60% and the transient period lengthens about 50 s.

Keywords: Numerical simulation, CO_2, gas cooler, transient behavior, thermophysical properties.

Resumen

Se investiga numéricamente el comportamiento transitorio del CO_2 dentro del enfriador de gas durante condiciones variables en el arranque de un sistema de refrigeración transcrítico. El análisis se basa en tres casos incluyendo: arranque en frío y en caliente con un flujo másico inicial de refrigerante de cero, y un arranque en caliente con un flujo másico nominal de CO_2. El análisis numérico es desarrollado usando un modelo 3D y simulaciones llevadas a cabo usando el código CFD FLUENT. Se analizan los efectos del cambio transitorio en las condiciones de frontera de entrada al enfriador de gas como temperatura, flujo másico, propiedades termofísicas, parámetros de transferencia de calor y efectividad térmica. Los resultados muestran que, cuando el sistema de refrigeración arranca a una alta temperatura y flujo másico nominal, la máxima efectividad térmica del enfriador de gas es del 85%. Cuando se arranca a alta temperatura con un flujo másico inicial de cero, la efectividad térmica decrece hasta un 60% y el periodo transitorio se alarga unos 50 s.

Palabras clave: Simulación numérica, CO_2, enfriador de gas, comportamiento transitorio, propiedades termofísicas.

1 Introduction

The start-up of refrigeration and air conditioning systems is an interesting transient process, in which the refrigerant mass flow rate and the temperature at the inlet and outlet of each component vary significantly. Refrigerant mass migration and redistribution across the components of the system are important factors influencing the transient and the cycling performance during the start-up operations (Li and Alleyne, 2010). The refrigerant mass has to migrate from the low-pressure components (evaporator and accumulator) to the high-pressure components (condenser and liquid tube) during the start-up.

* *Corresponding author. E-mail*: jfbelman@ugto.mx
Tel. 464 6479940 Ext. 2419
https://doi.org/10.24275/uam/izt/dcbi/revmexingquim/2019v18n3/Ituna
issn-e: 2395-8472

In the condenser, only about 19% of the total refrigerant mass of the system is located prior to start-up. This causes the transient period of the refrigerant mass migration to be longer, about one minute, in the condenser compared to the compressor and the evaporator (Peuker and Hrnjak, 2009). Similar results have been found by Li *et al*. (2010), in the study implemented on refrigerant migration modeling during the transient shutdown and start-up cycling operation. Recently, Li *et al*. (2018) concluded in their investigation on the cooling performance of a R410A split air conditioner during start-up by actively controlling refrigerant mass migration that by increasing the refrigerant mass in the condenser can improve cooling performance during start-up.

In most refrigeration and air conditioning systems the temperature is used as a control parameter to start-up and shutdown the compressor in order to guarantee a certain design requirement, such as the temperature in the compartments of a household refrigerator (Link and Deschamps, 2011). Xie and Bansal (2000) proposed a global simulation model for a hermetic reciprocating compressor in a conventional vapor compression system. They numerically simulate the transient behavior of pressure, temperature and velocity, as well as the heat transfer between the refrigerant and each part of the compressor domain during the start-up. Results showed significant variations of temperature in the refrigerant filling in the space between the shell and the compressor during the first 100 s of system start-up. From the simulation results, they suggested that, the coefficient of performance (COP) of a compressor obtained normally at steady state operation should be replaced by the mean value of integrating the transient function of COP. Browne and Bansal (2002) presented a transient model to predict the dynamic behavior of vapor compression liquid chillers. Transient behavior of cooling capacity, compressor work input, refrigerant temperatures in the evaporator and the condenser were analyzed during the start-up. Results showed that the refrigerant temperature in the condenser is greatly unsteady during the first 300 s of start-up, compared with the refrigerant temperature in the evaporator and with the compressor work input in which a small variation was noticeable in the first 200 s. Wu *et al*. (2016) developed an experimental investigation on cold start-up characteristics of a rotary compressor in a R290 air-conditioning system under cooling condition. The transient behavior of the suction and discharge temperature of the compressor was investigated. Results showed that the discharge temperature (which is also the condenser inlet temperature) is more unsteady in the first 400 s of start-up than the suction temperature. Therefore, it can be concluded from previous research that the condenser is the component most affected by the unsteadiness of the refrigerant mass and temperature during the start-up of vapor compression refrigeration systems.

In the CO_2 transcritical refrigeration system, the condenser is substituted by the gas cooler, where the carbon dioxide is cooled without any phase change process. Several studies carried out on this refrigeration system have led to the conclusion that the gas cooler is the component most affected by the unsteadiness in the thermophysical properties and the heat transfer when the system operating conditions are variable (Yoon *et al*., 2003; Li, 2013; Ge *et al*., 2015; Kim *et al*., 2017). These variations are much more pronounced when the system is in a transient state (Ituna-Yudonago and Belman-Flores, 2015). Although it is true that the instability is more accentuated in the gas cooler during the transient period of system operation, there is no study in the literature that can provide detailed information on these behaviors, especially during the start-up process. He *et al*. (2017) studied an optimal multivariable controller for transcritical CO_2 refrigeration cycle with an adjustable ejector. They investigated the behavior of gas cooler pressure during start-up, but no information was provided on other variables such as refrigerant temperature and refrigerant mass flow rate. Similarly, in the study conducted by Zheng *et al*. (2016) on the dynamic simulation of an improved transcritical CO_2 ejector expansion refrigeration cycle, apart from the detailed results provided on the ejector transient behavior, only the CO_2 pressure in the gas cooler was analyzed during the transient period. In the study performed by Belman-Flores *et al*. (2017) on the comparative analysis of a concentric straight and a U-bend gas cooler configurations in a CO_2 refrigeration system, the transient behavior of total heat transfer rate and thermal effectiveness in both concentric straight and U-bend gas coolers was investigated, but, no detailed information was provided on the refrigerant temperature, refrigerant mass flow rate transient behaviors. Ituna-Yudonago and Belman-Flores (2015) performed a study on the thermophysical properties of R744 in the supercritical region during the start-up of gas cooling process. Despite the interesting results obtained, this study was only focused on one start-up condition.

Based on the above, this paper provides new detailed information on the transient behavior of CO_2 in the gas cooler under cold and warm start-up conditions of a transcritical refrigeration system. The refrigerant temperature and the mass flow rate are the main conditions based on which this analysis is performed, since they are the most sensitive operating conditions during the start-up process of vapor compression refrigeration systems. The main contribution of this work is that it shows in detail how transient changes in the CO_2 temperature and the mass flow rate at the inlet of the gas cooler can affect the behavior of all thermophysical properties, the heat transfer and the thermal effectiveness of the gas cooler during the CO_2 transcritical refrigeration system start-up. The analysis is performed using a 3D model in order to have more information on the behavior of the heat transfer parameters in the whole volume of each domain. The numerical simulations are carried out using the commercial Computational Fluid Dynamics (CFD) code FLUENT.

2 Materials and methods

2.1 *Description of the gas cooler*

The gas cooler under study is a horizontal concentric CO_2/water U-bend heat exchanger, designed for an experimental refrigeration facility whose sketch is presented in Fig. 1. It is constituted of nineteen inner tubes through which CO_2 coming from the compressor (point 2) flows under supercritical conditions. The inner tubes are enclosed in an annular tube wherein the cold-water flows in the opposite direction, as subcooled liquid.

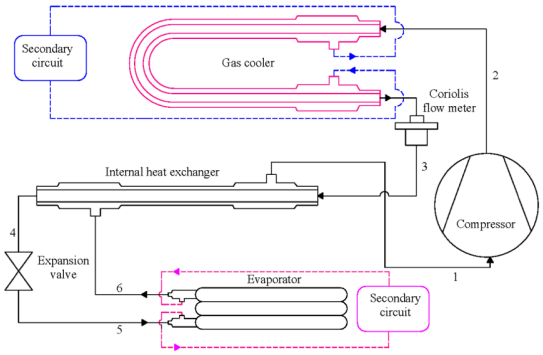

Fig. 1. Gas cooler location in the sketch of the transcritical refrigeration system.

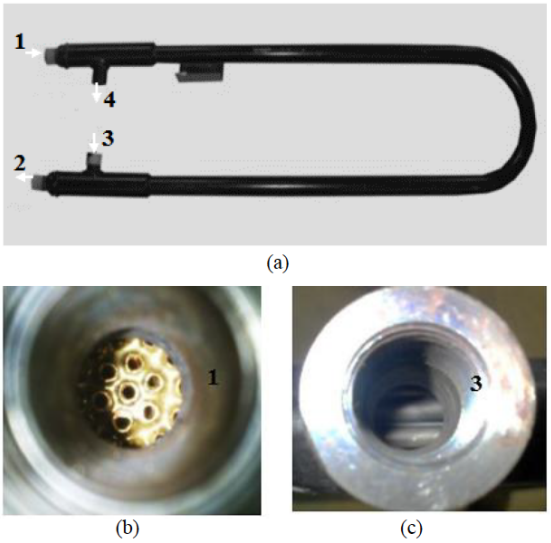

Fig. 2. Description of the concentric U-bend gas cooler: 1 → CO_2 inlet nozzle, 2→ CO_2 outlet nozzle, 3→Water inlet nozzle and 4→ Water outlet nozzle.

During the cooling process, the CO_2 transfers a large part of the heat to the water before entering the internal heat exchanger (point 3), where the rest of the heat is transferred to the CO_2 cold stream which exits the evaporator (point 6). Fig. 2 shows the different views of the concentric U-bend gas cooler. It can be seen from the top view (Fig. 2a) the geometric shape of the gas cooler as well as the location of the inlet and outlet nozzles of CO_2 and water streams. Fig. 2b shows the front view of the CO_2 inlet nozzle where some internal tubes are visible, and Fig. 2c shows the front view of the water inlet nozzle from the annular tube.

The general dimensions of the experimental U-bend gas cooler are described in Table 1; the inner tubes and the annular tube are made of stainless steel.

Table 1. Characteristics of the concentric U-bend gas cooler.

Item	Parameter	Size
Inner tube	Inner diameter [m]	0.00375
	Outer diameter [m]	0.005
	Average length [m]	2
	Number of tubes	19
Annular tube	Inner diameter [m]	0.03
	Outer diameter [m]	0.034
	Total length [m]	2
	Curvature radio [m]	0.112

2.2 *Design of the geometric model*

The geometric model is built in 3D using the ANSYS DesignModeler tool of the ANSYS Workbench platform according to the characteristics of the gas cooler. Additionally, some considerations were taken into account to reduce the complexity of the model:

- The geometric model is designed as tube-in-tube heat exchangers by considering an equivalent diameter (d_{eq}), which is the approximate inner diameter with a volume equal to that of the gas cooler. It is calculated by the Eq. (1) (Sánchez *et al*., 2012).

$$d_{eq} = d_i \cdot N_{tb}^{0.5} \tag{1}$$

  where d_i and N_{tb} are the diameter of tube and the number of tubes, respectively.

- The domain of the annular tube is not considered because there is no heat loss to the environment, i.e., the gas cooler is considered isolated.

Table 2 describes the geometric characteristics of the model and Fig. 3 shows its design. In Fig. 3a, the complete geometry is presented, while in Fig. 3b a front view of the model is shown. This figure allows the visualization of the three different domains including the CO_2 (1), the inner tube (2) and the water (3).

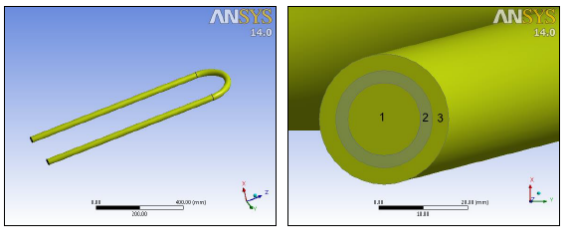

(a) (b)

Fig. 3. Concentric U-bend geometric model.

Table 2. Characteristics of the geometric model.

Item	Parameter	Size
Inner tube	Inner diameter [m]	0.01635
	Outer diameter [m]	0.02179
Annular tube	Inner diameter [m]	0.02916
	Curvature radio [m]	0.1120
	Length of the straight region [m]	0.8248
	Total length [m]	2

2.3 *Mathematical model*

The mathematical model is based on 3D transient equations of mass, momentum, energy, turbulent kinetic energy, and turbulence dissipation rate. The turbulent kinetic energy and turbulence dissipation rate equations are based on realizable $k-\varepsilon$ model which is proved to be a suitable model for simulating turbulent flow in the gas cooler (Yuan *et al*., 2015).

The following assumptions are taken into account in the mathematical modeling of the gas cooler:

- The gas cooler is considered isolated. So, all the heat removed from the refrigerant is transferred to the water.
- There is no phase change and no mass transfer in CO_2 during the gas cooling process.
- The governing equations are conserved.
- The gravitational force in the axial and angular direction is neglected.
- There is no volumetric heat source and no species diffusion.
- Pressure term in energy equation is neglected.

The governing equations are formulated as follows:
Mass conservation equation:

$$\frac{\partial \rho}{\partial t} + \nabla(\rho v) = 0 \tag{2}$$

Momentum conservation equation:

$$\frac{\partial(\rho v)}{\partial t} + \nabla \cdot (\rho v T) = \nabla(\mu \nabla v) - \nabla P + \rho g \tag{3}$$

Energy conservation equation:

$$\frac{\partial(\rho T)}{\partial t} + \nabla \cdot (\rho v T) = \nabla\left(\frac{\lambda}{C_p}\nabla T\right) + \Psi \tag{4}$$

Turbulent kinetic energy:

$$\frac{\partial}{\partial t}(\rho k) + \frac{\partial}{\partial x_i}(\rho k v_i) = \frac{\partial}{\partial x_j}\left[\left(v + \frac{v_i}{\sigma_k}\frac{\partial k}{\partial x_j}\right)\right] + P_k + P_b - \rho\varepsilon - Y_M + S_k \tag{5}$$

Turbulence dissipation rate:

$$\frac{\partial}{\partial t}(\rho\varepsilon)+\frac{\partial}{\partial x_i}(\rho\varepsilon v_i)=\frac{\partial}{\partial x_j}\left[\left(\nu+\frac{\nu_i}{\sigma_\varepsilon}\frac{\partial\varepsilon}{\partial x_j}\right)\right]+\rho C_1 S_\varepsilon - \rho C_2\frac{\varepsilon^2}{k+\sqrt{\nu\varepsilon}}+C_{1\varepsilon}\frac{\varepsilon}{k}C_{3\varepsilon}P_b+S_\varepsilon \quad (6)$$

In Eqs. (5) and (6), P_k represents the generation of turbulent kinetic energy due to the gradients of average velocity. P_b is the generation of turbulent kinetic energy due to buoyancy. Y_M is the viscous destruction and S_k, S_ε are source terms. Both coefficients are calculated in the same way as the standard $k-\varepsilon$ model. In addition, the coefficients in Eqs. (5) and (6) are defined according to (FLUENT, 2006) as follows:

$$C_{1\varepsilon}=1.44;\ \ C_2=1.9;\ \ \sigma_k=1.0;\ \ \sigma_\varepsilon=1.2$$

$$C_1=max\left[0.43,\frac{\eta}{\eta+5}\right] \quad (7)$$

$$\eta=S\frac{k}{\varepsilon} \quad (8)$$

where

$$S=\sqrt{2S_{ij}S_{ij}} \quad (9)$$

On the other hand, the turbulent viscosity is expressed by (FLUENT, 2006):

$$\nu_t=\rho C_\nu\frac{k^2}{\varepsilon} \quad (10)$$

$$C_{nu}=\frac{1}{A_0+A_s\frac{kU^*}{\varepsilon}} \quad (11)$$

In Eq. (11):

$$U^*\equiv\sqrt{S_{ij}S_{ij}+\Omega_{ij}\Omega_{ij}} \quad (12)$$

$$\Omega_{ij}=\Omega_{ij}-2\varepsilon_{ijk}\omega_k \quad (13)$$

$$\Omega_{ij}=\overline{\Omega}_{ij}-\varepsilon_{ijk}\omega_k \quad (14)$$

where $\overline{\Omega}_{ij}$ is the average rate rotation tensor in a reference frame rotating with the angular velocity ω_k. Constants A_0 and A_s are given by (FLUENT, 2006):

$$A_0=4.04$$

$$A_s=\sqrt{6}\cos\phi$$

$$\phi=\frac{1}{3}\cos^{-1}\left(\sqrt{6}W\right) \quad (15)$$

where

$$W=\frac{S_{ij}S_{jk}S_{ki}}{S^3} \quad (16)$$

$$S=\sqrt{S_{ij}S_{ij}} \quad (17)$$

$$S_{ij}=\frac{1}{2}\left(\frac{\partial u_j}{\partial x_i}+\frac{\partial u_i}{\partial x_j}\right) \quad (18)$$

2.4 *Boundary and initial conditions*

As previously described, the gas cooler consists of two streams including the refrigerant (CO_2) stream and the secondary fluid (water) stream. According to the start-up mode of the system under study, it is recommended that the operating conditions in the secondary circuits be in steady state before starting the main circuit composed of compressor, gas cooler, valve expansion, evaporator, and connection accessories. For this reason, the boundary conditions of the secondary fluid stream are constant. However, for the refrigerant stream, three different cases of boundary conditions are analyzed in this study. The first two cases are related to the start-up conditions of the transcritical refrigeration system under study, while the last case is correlated to the transient behavior of CO_2 during the cooling process in the gas cooler. Temperature and mass flow rate are the two variable operating conditions on which this analysis is performed. The proposed CO_2 stream boundary conditions are graphically shown in figs. 4a and 4b for the inlet temperature and inlet mass flow rate, respectively. The data base on which these graphics are built derive from a previous study conducted in (Pérez-García, 2014).

The behavior of each of the three cases is described as follows:

Case 1

This case is related to the cold start-up of the transcritical refrigeration system. When the system is turned off, the mass flow rate in the whole system is zero and the CO_2 temperature is around room temperature.

Table 3. Inlet boundary conditions (Pérez-García, 2014).

Case	CO_2		Water	
	Temperature [K]	Mass flow rate [kg s^{-1}]	Temperature [K]	Mass flow rate [kg s^{-1}]
1	305.36 - 405.7	0 - 0.036	298	0.441
2	405.7	0 - 0.036	298	0.441
3	405.7	0.036	298	0.441

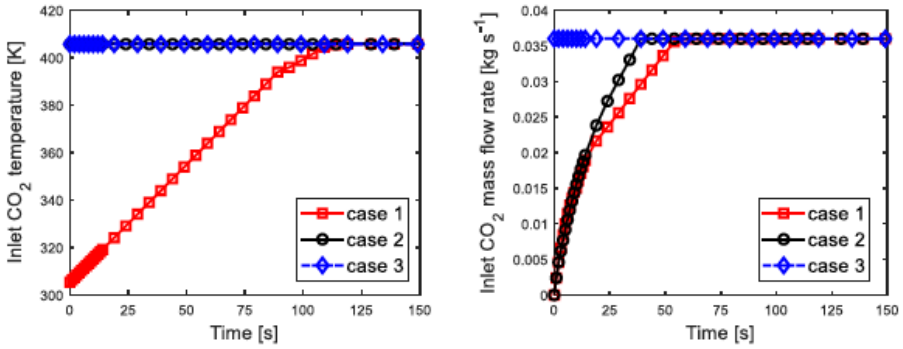

Fig. 4. Inlet temperature and mass flow rate behavior.

Therefore, during the start-up, the temperature at the entrance of the gas cooler begins to increase from the critical value (about 305.6 K) until reaching steady state at around 405.7 K, approximately after 110 s (see Fig. 4a). This temperature increase is caused by the compressor. At the same time, the CO_2 mass flow rate begins to increase due to the compression effect, but it quickly reaches steady state at around 0.036 kg s^{-1}, after 60 s (see Fig. 4b).

Case 2

The second case corresponds to the warm start-up of the transcritical refrigeration system, in which the system is restarted after a short stop. This case differs from the first one in the sense that, the temperature at the inlet of gas cooler remains around its steady value (405.7 K), but the mass flow is annulled due to system shutdown. During the system restart, the mass flow rate increases from 0 to 0.036 kg s^{-1} in approximately 40 s. It can be said that this case is the most common in the operation of vapor compression refrigeration systems, since the compressor must stop each time when there is no heat load in the refrigerator.

Case 3

This case is similar to the previous one, but the only difference is that the system starts under a nominal refrigerant mass flow rate. It corresponds to the simple observation of transient phenomena that can occur in the gas cooler during normal operation of the system when the CO_2 temperature and the mass flow rate at the inlet of the gas cooler remain constant. This case is a reference for the first two previous cases, since it allows measuring the degree of discrepancy that each case can present. A summary of the three cases described above is provided in Table 3.

Based on the behavior of CO_2 temperature and mass flow rate inlet boundary conditions, and considering that the CO_2 pressure at the gas cooler inlet remains constant around 9×10^6 Pa, the behavior of CO_2 density and viscosity at the gas cooler inlet are calculated using REFPROP dynamic libraries linked to Matlab (Lemmon *et al.*, 2007).

Fig. 5 shows the behavior of each property where it can be observed in figs. 5a and 5b that CO_2 density and viscosity decrease during the cold start-up (Case 1) due to the increase in temperature. In figs. 5c and 5d, the inlet CO_2 velocity and Reynolds number increase in cases 1 and 2 because of the growth in mass flow rate during start-up. In Case 3, there is no change because the temperature and the mass flow are constant. The trend of Reynolds number leads to conclude that the flow regime in the gas cooler is turbulent, since the steady state value of the Reynolds number is about 13×10^4.

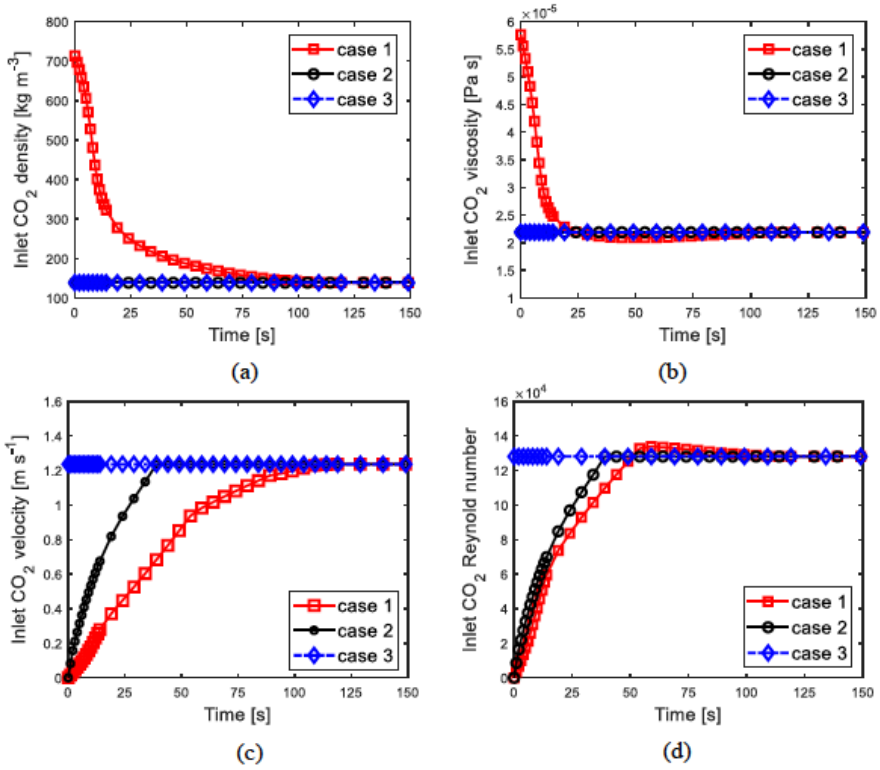

Fig. 5. Transient behavior of density, viscosity, velocity and Reynolds number at the inlet of the gas cooler.

These transport properties as well as the Reynolds number allow to analyze the behavior of the turbulent inlet boundary conditions such as the turbulent kinetic energy and the turbulent dissipation rate. These turbulence boundary conditions are calculated using the formula developed in (FLUENT, 2006). The turbulent kinetic energy (k) and the turbulence dissipation rate (ε) are calculated from Eqs. (20) and (21), respectively.

$$k = 0.0384u^2Re^{-1/4} \tag{19}$$

$$\varepsilon = \frac{C^{3/4}k^{3/2}}{l} \tag{20}$$

Where u and Re are the velocity and the Reynolds number of CO_2 at the gas cooler inlet. C is an empirical constant specified in the turbulence model, approximately 0.09, and l is the turbulence length scale, in this case $l = 0.07d_i$. The trends of these boundary conditions are shown in Fig. 6. It can be observed that the behavior of the turbulent kinetic energy (Fig. 6a) and the turbulence dissipation rate (Fig. 6b) are much more influenced by the CO_2 velocity.

On the other hand, in previous studies it has been shown that the pressure of CO_2 and water at the outlet of the cooler gas does not change much during the transient period. Therefore, in this work the pressure is proposed as an exit boundary condition. The water stream boundary conditions are described in Table 4 below.

The initial conditions correspond to the initial state of each case at the moment of start-up. The details for each case are presented in Table 5.

Table 4. Table 4. Water stream boundary conditions.

Boundary	Description	Value
Water inlet	Mass flow rate [kg s-1]	0.441
	Temperature [K]	298
Water outlet	Pressure [Pa]	1.5×10^5
	Backflow total temperature [K]	300
	Thermal condition	Adiabatic
Outer wall	Wall motion	Stationary
	Shear condition	No slip

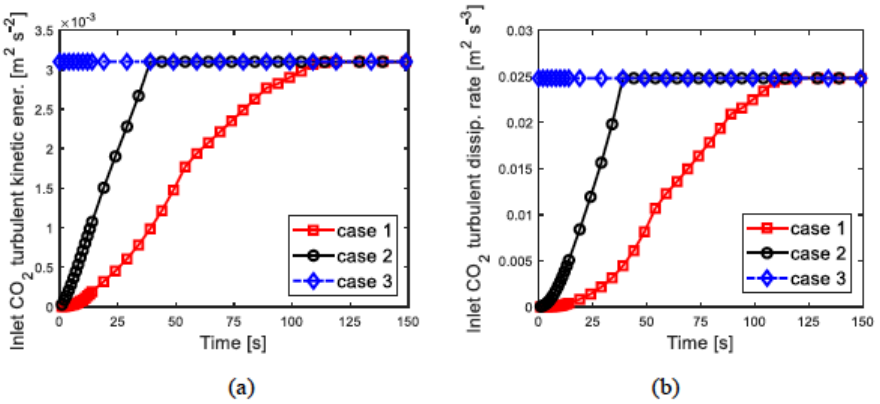

Fig. 6. Transient behavior of turbulent kinetic energy and the turbulence dissipation at the inlet of the gas cooler.

Table 5. Initial conditions for the three cases (Pérez-García, 2014).

Case	CO_2			Water		
	Temperature [K]	Pressure [Pa]	Mass flow rate [kg s^{-1}]	Temperature [K]	Pressure [Pa]	Mass flow rate [kg s^{-1}]
1	305.36	9×10^6	0	298	1.5×10^5	0.441
2	405.7	9×10^6	0	298	1.5×10^5	0.441
3	405.7	9×10^6	0.036	298	1.5×10^5	0.441

2.5 *Mesh independence analysis*

In this section the meshing requirements to validate the results are shown. It is important to remember that the numerical solution may be dependent on the grid density. In this study, the mesh is performed in ANSYS Meshing. The unstructured sweep method with all tri free face mesh-type is chosen in order to have the control on the cell size near the interfaces of the different domains. Fig. 7a shows the mesh in real geometry size, while Fig. 7b shows a zoomed view to better observe the quality of the mesh.

The mesh independence analysis is carried out by varying the mesh size as shown in Fig. 8. The temperature of the CO_2 is considered to be the parameter on which the sensitive analysis of the mesh is performed. This choice is due to the fact that temperature is the main operating condition in which a small change can significantly affect the behavior of the thermophysical properties and therefore the heat transfer rate (Yoon *et al.*, 2003; Ge *et al.*, 2015). The analysis is performed using six different mesh sizes as shown in Fig. 8. Simulation of these six models is carried out considering the boundary and initial conditions for Case 3 previously described.

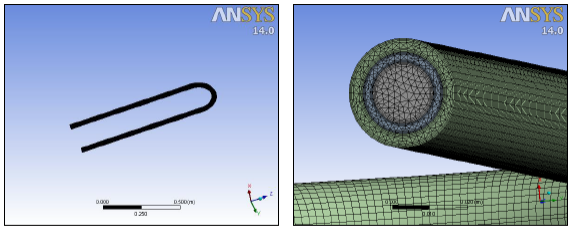

Fig. 7. Meshing model.

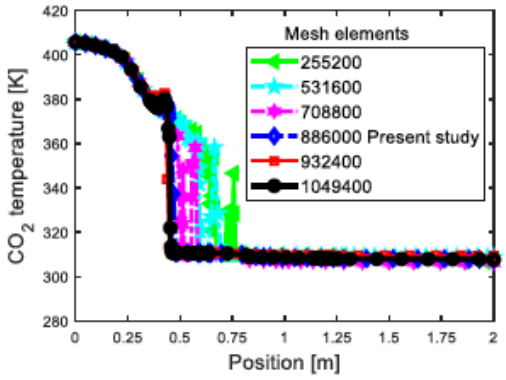

Fig 8. Mesh independence analysis.

Table 6. Mesh characteristics of the geometric model.

Item		Size
Nodes		715715
Elements		886000
Orthogonality	Minimum	0.3650
	Maximum	0.9993
Skewness	Minimum	0.0019
	Maximum	0.7132

The results are presented along the gas cooler in the axial direction considering the average transversal value of the CO_2 temperature at each position, in order to test the mesh quality at different locations. It can be observed that the profiles of the temperature are no longer influenced by the mesh sizes when the number of mesh elements is greater than or equal to 886000. In order to reduce the computational time of simulation, the geometric model containing 886000 mesh elements is chosen for this study. The characteristics of the selected mesh sizes are presented in Table 6, where it can also be observed the quality control factors (orthogonality and skewness) which are in the recommended range.

2.6 *Numerical simulation procedure*

The simulation is performed using the commercial software ANSYS FLUENT. Thermophysical properties of CO_2 and water are considered to be dependent on temperature. These properties including specific heat, thermal conductivity, dynamic viscosity, density and Prandtl number for both CO_2 and water are obtained from REFPROP thermodynamic tables, written in the language C++ and linked to FLUENT through User Defined Functions (UDFs). SIMPLEC algorithm is adopted for pressure-velocity coupling, which is particularly recommended for the case of buoyant flows. The second order QUICK scheme is used for the discretization of the convective terms in the momentum, energy and turbulence equations. The adaptive time step is used by considering a range from 10^{-3} s to 10^{-5} s, for facilitating convergence and ensuring the accuracy of the solutions.

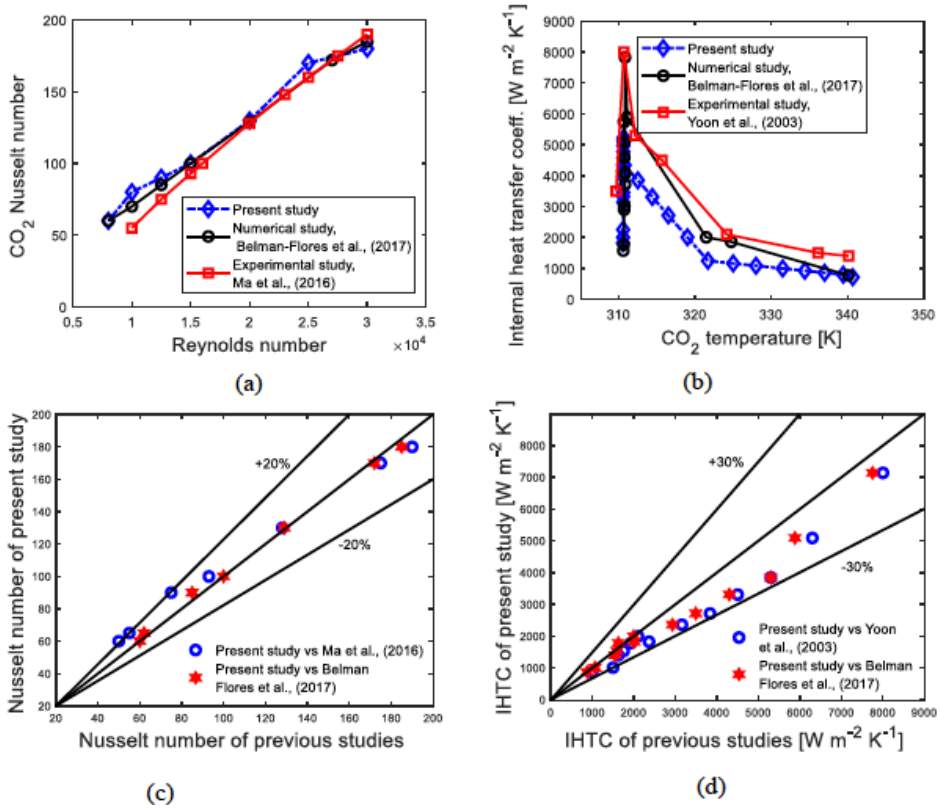

Fig 9. Comparison between predicted parameters and other studies: (a) Nusselt number; (b) Internal heat transfer coefficient; (c) Nusselt number relative errors; (d) Internal heat transfer coefficient relative errors.

2.7 *Comparison of some parameters with previous works in literature*

To ensure the reliability of the results of this study, a comparison of some results is made with those from theoretical and experimental works performed on gas cooler with characteristics and operating conditions similar to the present study. Note that the experimental facility on which this study is based, is stills under construction. Two experimental works carried out by Ma *et al*. (2016) and Yoon *et al*. (2003) and one numerical study performed by Belman-Flores *et al*. (2017) are chosen for this comparison. Numerical results of Case 3 are selected for this comparison, since the previous studies have been done considering constant boundary conditions. Fig. 9a shows the trends of the Nusselt number as a function of Reynolds number reported in the studies performed by Ma *et al*. (2016) and Belman-Flores *et al*. (2017) which are compared with the present study. On the other side, Fig. 9b presents the influence of the CO_2 temperature variation on the gas cooler internal heat transfer coefficient. The comparison is done between Yoon *et al*. (2003), Belman-Flores *et al*. (2017) and the present study. The relative errors between the results of the present study and those of the three previous works are presented in Fig. 9c and 9d, for the Nusselt number and the internal heat transfer coefficient (IHTC), respectively. It can be observed that the results of the predicted model present a good agreement with those of the three previous studies. The maximum error in the comparison of the Nusselt number is 20%. As for the comparison of the IHTC, the maximum error is 30%. The results of these comparisons give some confidence in the use of the present numerical model for predicting the behavior of the gas cooler.

3 Results and discussion

This section presents the simulation results of the gas cooler transient model described previously. Results are presented graphically in time including the three cases describing the transient average and outlet profiles of CO2 temperature, mass flow rate, thermophysical properties and the heat transfer parameters.

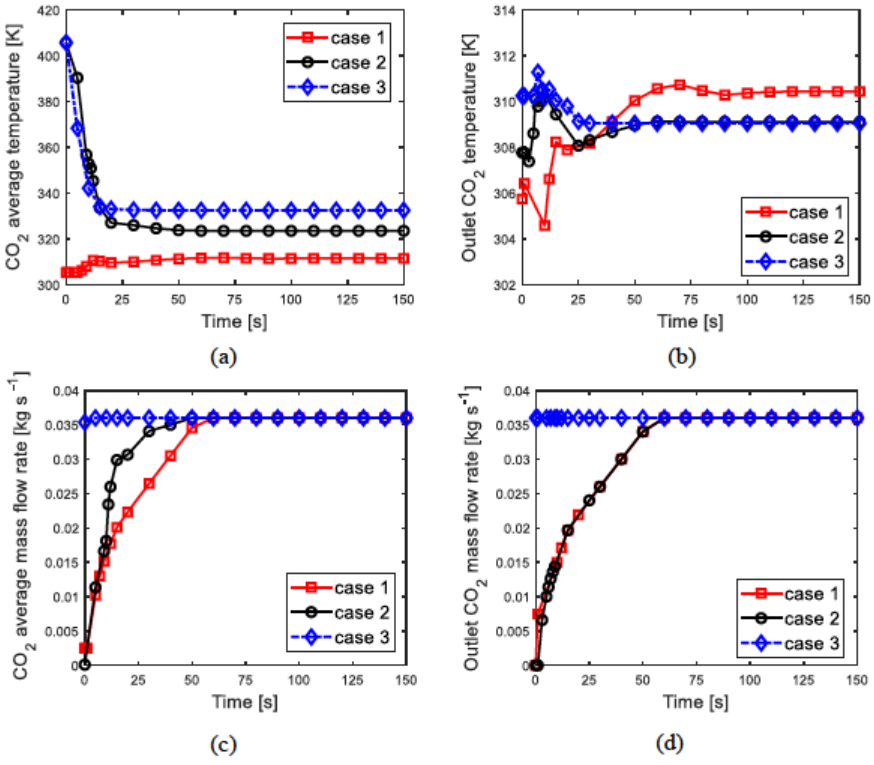

Fig. 10. Transient behavior of CO_2 temperature and mass flow rate inside and at the outlet of the gas cooler.

The average results allow to understand the heat transfer behavior of CO_2 inside the gas cooler during system startup, while the tendencies in the CO_2 properties at the exit of the gas cooler make it possible to have an idea of their influence on the other components, in particular the intermediate heat exchanger, whose heat transfer rate depends much more on the CO_2 properties at the outlet of the gas cooler (Ituna-Yudonago, 2017). The section ends by illustrating the temporal profiles of the thermal effectiveness of the gas cooler which plays an important role in the prediction of the COP of the whole transcritical refrigeration system. It should be noted that, the pressure behavior is not analyzed, since it does not present a significant variation in all three cases. Its magnitude is almost constant around 9×10^6 Pa.

3.1 Transient behavior of CO_2 temperature and mass flow rate

Temperature and mass flow rate are the main parameters of a fluid whose variation affects much more the heat transfer in a heat exchanger as previously described. This subsection describes the transient behavior of temperature and mass flow rate inside the gas cooler (average behavior) and at the outlet. Fig. 10a shows the temporal profile of CO_2 average temperature during the gas cooling process from the startup to the steady state, for the three cases. It can be observed that an important change occurred in the first 20 s. The most relevant variations are observed in Cases 2 and 3 due to their warm-starting conditions. The decrease in the CO_2 temperature is due to the cooling effect. The only difference between these two cases is the mass flow rate (see Table 3) which is the basis of the slight difference between their profiles. In Case 1 the average temperature increases from 305.36 K (inlet condition) to 310 K during the first 20 s, and continues to vary slightly until reaching steady state around 311 K, approximately after 120 s. The slight temperature variation in Case 1 occurs near the pseudo-critical value (311 K). On the other hand, the output CO_2 temperature behaves differently from previous trends. In the three cases, the temperature fluctuates between 304 K and 312 K. The low magnitude of the outlet temperature is due to the fact that CO_2 and water flow arrangement is counterflow in the gas cooler. During the transient period, the CO_2 temperature undergoes a more significant change at the exit of the gas cooler when the system starts in cold conditions (Case 1) than in warm conditions (Case 2 and 3). In addition, the outlet temperature in Case 1 reaches steady state around 310 K which is the pseudo-critical temperature.

In general, it appears from the analysis of the temperature trends inside and at the exit of the gas cooler that, Case 1, which corresponds to the cold start-up mode, could have a significant impact on the thermophysical properties of CO_2, since it has been shown in the literature that the thermophysical properties of CO_2 vary significantly when the temperature is supercritical (Belman-Flores *et al*., 2017; Ma *et al*., 2016; Bae, 2016; Eldik *et al*., 2014). Unlike temperature, the CO_2 mass flow rate does not vary significantly during the transition period, neither inside the gas cooler nor at the outlet, as shown in figs. 10c and 10d, respectively. The transient mass flow behavior inside the gas cooler (Fig. 10c) is very similar to that prescribed as the boundary condition at the inlet (Fig. 4b), while at the exit (Fig. 10d), negligible differences are observed between Cases 1 and 2.

3.2 Transient behavior of CO_2 thermophysical properties

The thermophysical properties such as density, specific heat, viscosity, thermal conductivity, thermal diffusivity, and Prandtl number are the most important properties of fluids that can allow understanding how the heat transfer behaves in a heat exchanger. Average and outlet trends of these thermophysical properties are shown in the Fig. 11. In general, Case 1 is that in which the thermophysical properties of CO_2 vary significantly. In figs. 11a and 11b, the density of CO_2 behaves differently in Case 1 compared to the other cases. These trends are strongly temperature dependent since it is well known that the density of a fluid (CO_2) decreases as its temperature increases. Either inside or at the outlet of the gas cooler, the important changes in CO_2 density occur when the temperature of CO_2 is in the pseudo-critical region. The same observation is made in the behavior of the viscosity of CO_2 which is strongly related to the density, as shown in figs. 11c and 11d. Specific heat is the property most affected by the change when the CO_2 temperature is pseudo-critical. This can be seen in figs. 11e and 11f. The average specific heat (Fig. 11e) increases from almost 1200 J $kg^{-1}K^{-1}$ to 6800 J $kg^{-1}K^{-1}$ during the first 50 s in Case 2 which corresponds to the warm start-up mode.

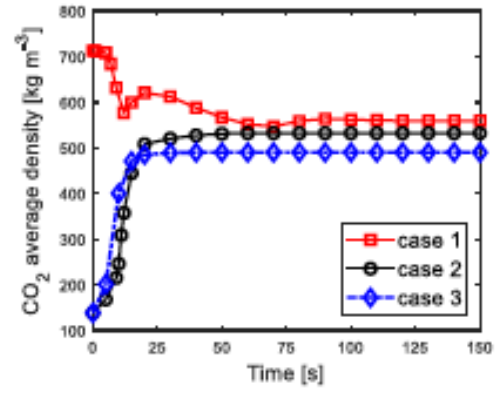
CO_2 average density [kg m^{-3}]
Time [s]
case 1
case 2
case 3

(a)

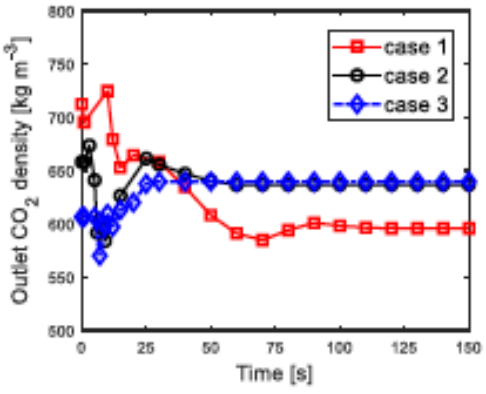
Outlet CO_2 density [kg m^{-3}]
Time [s]
case 1
case 2
case 3

(b)

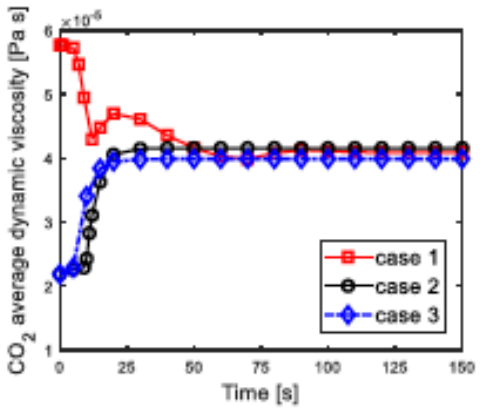
CO_2 average dynamic viscosity [Pa s]
Time [s]
case 1
case 2
case 3

(c)

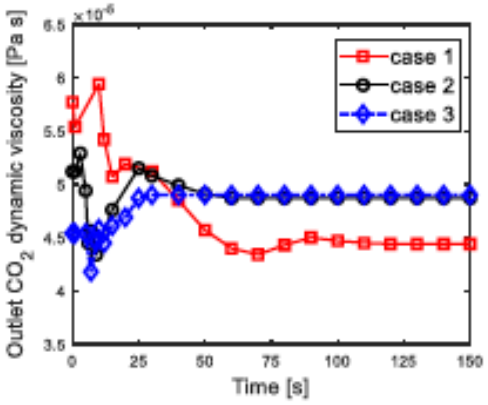
Outlet CO_2 dynamic viscosity [Pa s]
Time [s]
case 1
case 2
case 3

(d)

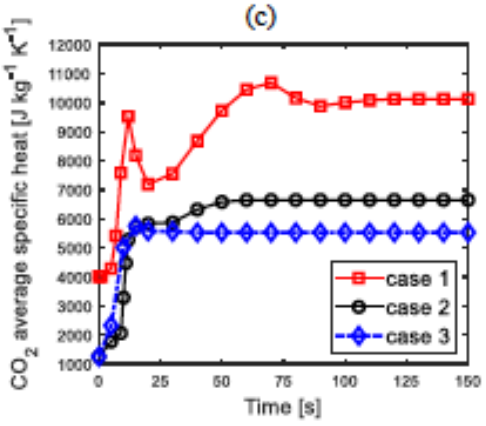
CO_2 average specific heat [J kg^{-1} K^{-1}]
Time [s]
case 1
case 2
case 3

(e)

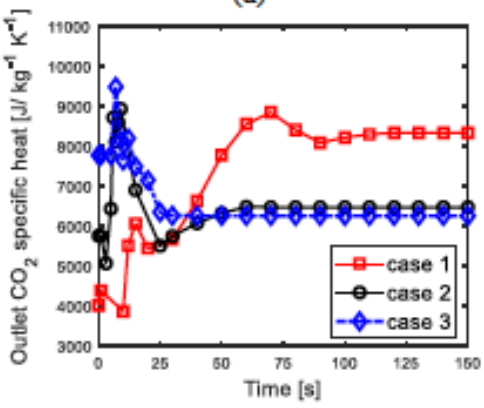
Outlet CO_2 specific heat [J/ kg^{-1} K^{-1}]
Time [s]
case 1
case 2
case 3

(f)

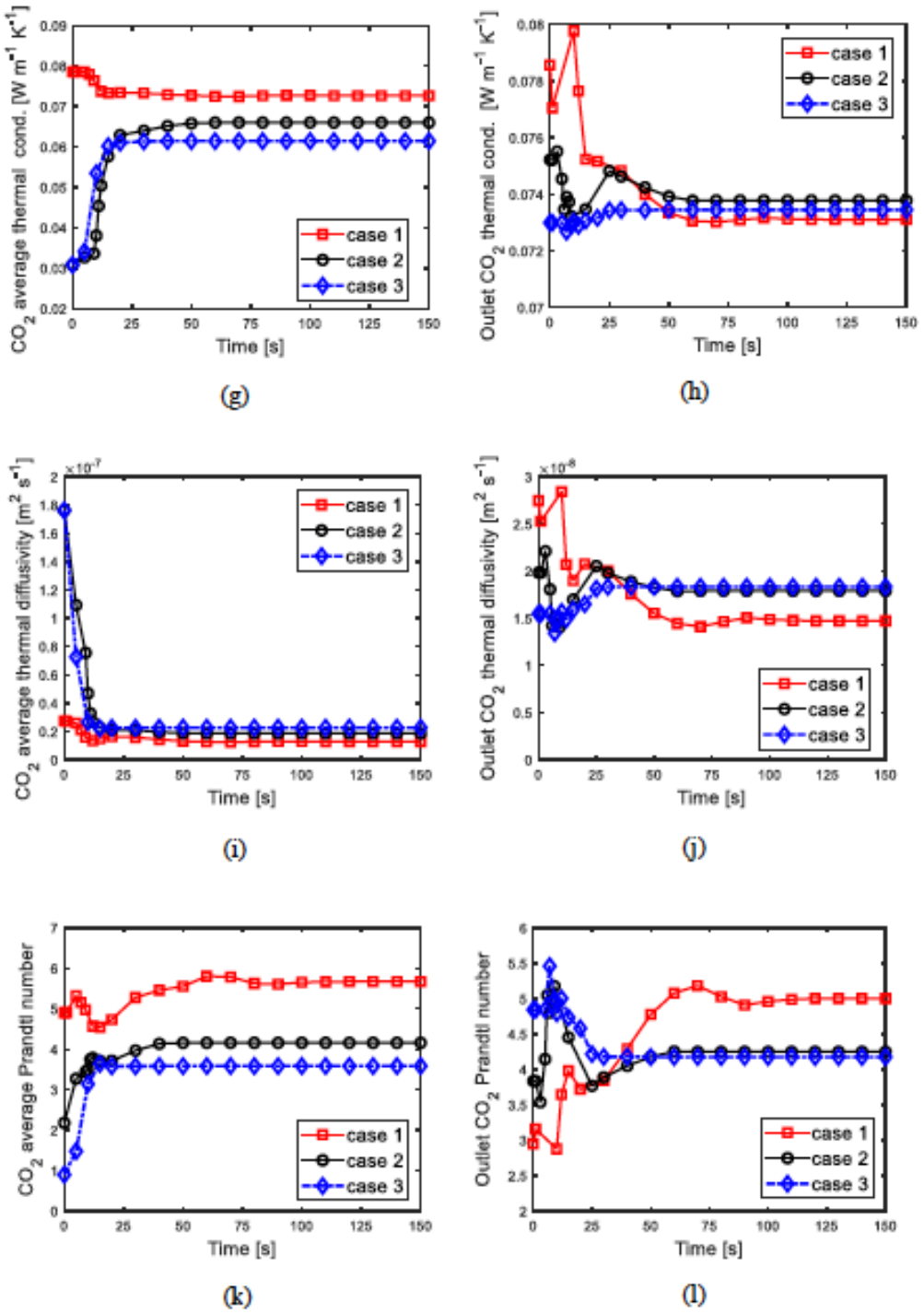

Fig. 11. Transient behavior of CO2 thermophysical properties inside and at the outlet of the gas cooler.

This behavior is almost similar in Case 3 but, the only difference is that the transient period is very short (about 15 s) and also the magnitude of the specific heat in the steady state is low (5500 J $kg^{-1}K^{-1}$). The cold start-up mode (Case 1), is characterized by a large change in specific heat. The average specific heat changes from 4000 J $kg^{-1}K^{-1}$ at the initial condition and increases while varying up to 10000 J $kg^{-1}K^{-1}$,

during the first 100 s. The difference at the steady state between the specific heat of Case 1 and 2 is 3200 J $kg^{-1}K^{-1}$, approximately 32%. This is because the CO_2 temperature in Case 1 is in the pseudo-critical region. The difference in magnitude of the specific heat between the two starting modes can lead to a large difference in the thermal effectiveness of the gas cooler, due to the relationship between specific heat and thermal effectiveness during gas cooling process (Belman-Flores *et al*., 2017). At the gas cooler exit (Fig. 11f), the trends of the specific heat are almost similar (Cases 2 and 3), especially in the steady state region, but, the significant variations observed in Cases 2 and 3 during the transient period are due to the fact that the CO_2 temperature at a time of 15 s is in the pseudo-critical region as previously shown in Fig. 10b.

Thermal conductivity is another thermophysical property whose behavior allows predicting the heat transfer rate. Its average and outlet behaviors are shown in figs. 11g and 11h, respectively. It can be observed in the three cases that CO_2 has a high thermal conductivity in the gas cooler when its temperature is low. The most relevant case is the cold start-up (Case 1), where the magnitude of the CO_2 thermal conductivity is higher during the transient period, due to the low start-up temperature compared to Cases 2 and 3, as previously shown in Fig. 10a and 10b. However, the low CO_2 thermal conductivity at the outlet (Fig. 11h), in Case 1, could negatively affect the thermal effectiveness of the gas cooler. This behavior can be better understood by analyzing the thermal diffusivity of CO_2 in the gas cooler, which is the main thermophysical property that measures the ability of a material to conduct thermal energy relative to its ability to store thermal energy. The trends of thermal diffusivity inside the gas cooler (Fig. 11i) and at the exit (Fig. 11j), lead to predict that, cold start-up can result in lower heat transfer rate in the gas cooler. These results can also be confirmed by analyzing the behavior of the Prandtl number, which is a dimensionless parameter representing the ratio of diffusion of momentum to the diffusion of heat in a fluid. It can be used to determine the heat transfer rate in fluid. As shown in figs. 11 k and 11l, the high magnitude of Prandtl number in Case 1 means that heat transfer rate is lower.

Another aspect that can attract attention is that of the effect of the CO_2 specific heat on the thermal diffusivity and the Prandtl number in the gas cooler. As previously shown in Fig. 11e and 11f, the CO_2 specific heat undergoes a significant increase in Case 1, due to the fact that, the CO_2 temperature is near the pseudo-critical value. This increase causes a decrease in thermal diffusivity (Case 1, Fig. 11i and 11j) and an important increase in the Prandtl number (Case 1 Fig. 11k and 11l). This leads to the conclusion that, CO_2 specific heat is the most important thermophysical property in the gas cooler. Its behavior can allow predicting the CO_2 heat transfer rate during the gas cooling process.

3.3 *Transient behavior of gas cooler heat transfer parameters*

Transient behavior of gas cooler inner heat transfer flux and heat transfer rate are shown in figs. 12a and 12b, respectively. These two parameters have almost the same trend, due to the fact that they are closely related.

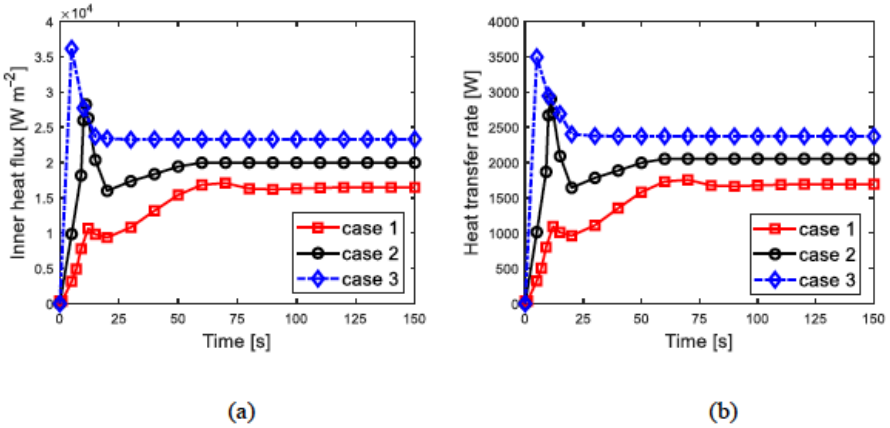

Fig. 12. Transient behavior of heat transfer parameters: (a) Inner heat flux; (b) heat transfer rate.

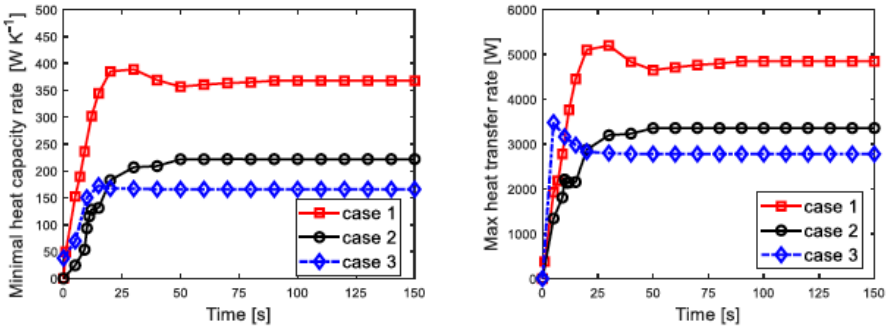

(a) (b)

Fig. 13. Transient behavior of the gas cooler minimal heat capacity rate and maximum possible rate of heat transfer.

The transient period is characterized by similar changes in all three cases. Cases 2 and 3, experienced a significant increase in heat flux and heat transfer rate in the first 20 s of system startup, due to the high level of start-up temperature. However, in Case 3 the fluctuations stabilize around a heat flux of 2.4×10^4 Wm^{-2} (Fig. 12a) and a heat transfer rate of 2400 W (Fig. 12b), since this case matches a simple observation of transient effects during the cooling process. Case 1 is characterized by a lower heat transfer flux and heat transfer rate as previously predicted by analyzing the CO_2 thermal diffusivity and Prandtl number. By comparing Case 1 with Case 2, it appears that the heat transfer rate is about 20% lower for Case 1, and, in addition, its transient period is longer (about 100 s), which can cause a great instability in the gas cooler and therefore, the overall operation of the system.

3.4 *Transient behavior of the gas cooler thermal effectiveness*

The thermal effectiveness (eff) is a measure of the performance of a heat exchanger. Since it is not part of the fluent codes, its calculation is based on the ε-NTU method. As shown in Eq. (20), the thermal effectiveness is defined as the ratio of the current heat transfer rate (Q_{gc}) and the maximum possible rate of heat transfer ($Q_{max,gc}$).

$$\frac{Q_{gc}}{Q_{max,gc}} \tag{21}$$

where

$$Q_{max,gc} = C_{min}\left(T_{CO_2,i} - T_{water,i+1}\right) \tag{22}$$

In Eq. (21), the subscripts i and $i+1$ represent the current and backward node in the control volume, respectively. The notation $i+1$ refers to the backward node in the water stream side in the control volume because the water stream flows in the opposite direction to the CO_2 stream. C_{min} is the minimal heat capacity rate (i.e. mass flow rate multiplied by specific heat) between both CO_2 heat capacity rate and water heat capacity rate. Transient behavior of gas cooler minimal heat capacity rate and maximum possible rate of heat transfer are shown in Fig. 13a and 13b, respectively. In general, Case 1 is the most concerned by a large fluctuation and a high minimal heat capacity rate and maximum possible rate of heat transfer. This increase is strongly related to the behavior of the specific heat of CO_2 (figs. 11e and 11f) which is involved in the calculation of the minimal heat capacity rate.

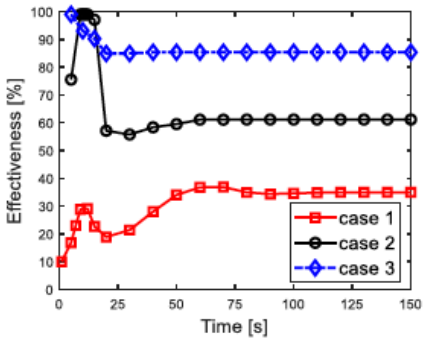

Fig. 14. Transient behavior gas cooler thermal effectiveness.

The higher maximum heat transfer rate can lead to a decrease in the thermal effectiveness of the gas cooler. That is clearly shown in Fig. 14, where Case 1 is characterized by a very low thermal effectiveness in comparison with the other two cases. The magnitude of the thermal effectiveness is almost half of that for Case 2. This lower thermal effectiveness is not only due to the higher magnitude of the maximum heat transfer rate, but also because of its low heat transfer rate (Fig. 12b). Additionally, the transient period in Case 1 is about two times longer than in Case 2. When the system starts in warm mode (Case 2), the gas cooler has a good performance. The thermal effectiveness reaches 60%, with a transient behavior during the first 50 s. During normal system operation (Case 3), the thermal effectiveness of the gas cooler reaches 85%. The high thermal effectiveness at the beginning, in Cases 2 and 3, is due to the slight thermal load, since the temperature of the refrigerant at start-up is high.

Particular attention should be made when the system starts in cold mode, since the low thermal effectiveness can lead to a low COP, because the gas cooler is the component whose performance has a great impact on the efficiency of the transcritical refrigeration system (Yoon *et al*., 2013; Kim *et al*., 2017; Ituna-Yudonago and Belman-Flores 2015).

Conclusions

Transient behavior of CO_2 in the gas cooler during variable start-up conditions of the transcritical refrigeration system was numerically investigated in this paper. The analysis was based on three cases including cold and warm start-up with zero initial refrigerant (CO_2) mass flow rate, and warm start-up with nominal CO_2 mass flow rate. The numerical analysis was performed using a 3D model and simulations were carried out using the commercial Computational Fluid Dynamics (CFD) code FLUENT.

In all three cases, transient behavior of CO_2 temperature, mass flow rate, thermophysical properties, heat transfer parameters and gas cooler thermal effectiveness have been analyzed in detail. The main conclusions of this study are summarized as follow:

- The transient behavior of CO_2 thermophysical properties in the gas cooler is much more affected by the variation in the CO_2 temperature than in the CO_2 mass flow rate, during the transcritical refrigeration system start-up.

- The specific heat thermophysical property is the most affected by the variation in the CO_2 temperature, during the transcritical refrigeration system start-up.

- Thermal effectiveness of the gas cooler reaches 85% when the transcritical refrigeration system starts at high temperature and nominal refrigerant mass flow rate.

- When transcritical refrigeration system starts at high temperature with zero initial CO_2 mass flow rate, the thermal effectiveness of the gas cooler decreases up to 60% and the transient period lengthens a bit (about 50 s).

- The low thermal effectiveness of the gas cooler during the cold start-up is attributed to the high CO_2 specific heat caused by the CO_2 temperature inside the gas cooler which remains around the pseudo-critical value.

Finally, particular attention should be made when the system starts in cold mode, since the low thermal effectiveness can lead to a low COP, because the gas cooler is the component whose performance has a great impact on the efficiency of the transcritical refrigeration system. Improving the thermal effectiveness of the gas cooler during cold start-up may be possible by increasing the temperature of the water at the inlet of the gas cooler secondary circuit to allow the increase in the CO_2 temperature.

Acknowledgements

The authors wish to thank the Directorate for Research Support and Postgraduate Programs at the University of Guanajuato for their support this research project.

Nomenclature

C_p	Specific heat, kJ kg^{-1}K^{-1}
D	Dimension
P	Pressure, Pa
T	Temperatura, K
t	Time, s
v	Velocity, m s^{-1}
X	Direction, m

Greek symbols

ρ	Density, kg m-3
μ	Dynamic viscosity, Pa s
λ	Thermal conductivity, W $m^{-1}K^{-1}$
ϕ	Angle, °
Ψ	Viscous dissipation

Subscripts

i	Coordinate index in x direction
j	Coordinate index in y direction
k	Coordinate index in z direction
t	Turbulent
μ	Viscosity

References

Bae, Y.Y. (2016). A new formulation of variable turbulent Prandtl number for heat transfer to supercritical fluids. *International Journal of Heat and Mass Transfer 92*, 792-806.

Belman-Flores, J.M., Ituna-Yudonago, J.F., Elizalde-Blancas, F., Serrano-Arellano, J., Morales-Fuentes, A. (2017). Comparative analysis of a concentric straight and a U-bend gas cooler configurations in CO_2 refrigeration system. *International Journal of Heat and Mass Transfer 106*, 756-766.

Browne, M.W., Bansal, P.K. (2002). Transient simulation of vapour compression packaged liquid chillers. *International Journal of Refrigeration 25*, 597 - 610.

Eldik, M., Harris, P.M., Kaiser, W.H., Rousseau, P.G. (2014). Theoretical and experimental analysis of supercritical carbon dioxide cooling. *International Refrigeration and Air Conditioning Conference paper 1360*.

FLUENT 6.3 User's Guide - 12.4 Standard, RNG, and Realizable, Fluent Inc. 2006-09-20. https://www.sharcnet.ca/Software/Fluent6/html/ug/node480.htm

Ge, Y.T., Tassou, S.A., Santosa, I.D., Tsamos, K. (2015). Design optimisation of CO_2 gas cooler/condenser in a refrigeration system. *Applied Energy 160*, 973-981.

He, Y., Deng, J., Yang, F., Zhang, Z. (2017). An optimal multivariable controller for transcritical CO_2 refrigeration cycle with an adjustable ejector. *Energy Conversion and Management 142*, 466 - 476.

Ituna-Yudonago, J.F., Belman-Flores, J.M. (2015). Thermophysical properties of R744 in supercritical region during the start-up of gas cooling process. *Revista Mexicana de Ingeniería Química 14* 213 - 229.

Ituna-Yudonago, J.F., Belman-Flores, J.M., Elizalde-Blancas, F., García-Valladares, O. (2017). Numerical investigation of CO_2 behavior in the internal heat exchanger under variable boundary conditions of the transcritical refrigeration system. *Applied Thermal Engineering 115*, 1063-1078.

Kim, M.S., Kang, D.H., Kim, M.S., Kim, M. (2017). Investigation on the optimal control of gas cooler pressure for a CO_2 refrigeration system with an internal heat exchanger. *International Journal of Refrigeration 77*, 48 -59.

Lemmon, E.W., McLinden, M.O., Huber, M.L. 2007. REFPROP NIST Standard Reference Database 23, v. 8.0. National Institute of Standards; Gaithersburg, Maryland 20899, USA.

Li, B., Alleyne, A. (2010). A dynamic model of a vapor compression cycle with shut-down and start-up operations. *International Journal of Refrigeration 33*, 538-552.

Li, B., Peuker, S., Alleyne, A., Hrnjak, P. (2010). Refrigerant migration modeling during shut-down and start-up cycling transients "Refrigerant migration modeling during shut-down and start-up cycling transients". *International Refrigeration and Air Conditioning Conference Paper 1092*. http://docs.lib.purdue.edu/iracc/1092.

Li, J., Deng, W., Yan, G. (2018). Improving quick cooling performance of a R410A split air conditioner during start-up by actively controlling refrigerant mass migration. *Applied Thermal Engineering 128*, 141-150.

Li, W. (2013). Optimal analysis of gas cooler and intercooler for two-stage CO_2 trans-critical refrigeration system. *Energy Conversion and Management 71*, 1-11.

Link, R., Deschamps, C.J. (2011). Numerical modeling of start-up and shutdown transients

in reciprocating compressors. *International Journal of Refrigeration 34*, 1398 - 1414.

Ma, T., Chu, W.X., Xu, X.Y., Chen, Y.T., Wang, Q.W. (2016). An experimental study on heat transfer between supercritical carbon dioxide and water near the pseudocritical temperature in a double pipe heat exchanger. *International Journal of Heat and Mass Transfer 93*, 379-387.

Peuker, S., Hrnjak, P.S. (2009). Transient Refrigerant and Oil Migration of an R134a Automotive A/C System. *SAE International Journal of Passenger Cars - Mechanical Systems 2*, 714-724.

Pérez-García, V. 2014. *Application of CO_2 in the Production of Cold: Dimensioning and Construction of a Transcritical Installation*. Ph.D. Thesis, University of Guanajuato, Mexico (in Spanish).

Sánchez, D., Cabello, R., Llopis, R., Torrella, E. (2012). Development and validation of a finite element model for water-CO_2 coaxial gas-coolers. *Applied Energy 93*, 637-647.

Wu, J., Lin, J., Zhang, Z., Chen, Z., Xie, J., Lu, J. (2016). Experimental investigation on cold start-up characteristics of a rotary compressor in the R290 air-conditioning system under cooling condition. *International Journal of Refrigeration 65*, 209 - 217.

Xie, G., Bansal, P.K. (2000). Dynamic simulation model of a reciprocating compressor in a refrigerator. In: *Proceedings of the International Compressor Conference at Purdue*, West Lafayette, IN, 129 - 136.

Yoon, S.H., Kim, J.H., Hwang, Y.W., Kim, M.S., Min, K., Kim, Y. (2003). Heat transfer and pressure drop characteristics during the in-tube cooling process of carbon dioxide in the supercritical region. *International Journal of Refrigeration 26*, 857-864.

Yuan, H., Edlebeck, J., Wolf, M., Anderson, M., Corradini, M., Klein, S., Nellis, G. (2015). Simulation of Supercritical CO_2 Flow Through Circular and Annular Orifice. *Journal of Nuclear Engineering and Radiation Science 1*, 2-11.

Zheng, L., Deng, J., Zhang, Z. (2016). Dynamic simulation of an improved transcritical CO_2 ejector expansion refrigeration cycle. *Energy Conversion and Management 114*, 278-289.